Separation and Purification Technology 379 (2025) 134917

Contents lists available at ScienceDirect

Separation and Purification Technology

journal homepage: www.elsevier.com/locate/seppur

β–Cyclodextrin polymerization for selective separation of long-chain per- and poly-fluorinated alkyl substances at environmentally relevant concentrations

Monu Verma [a,1], Youngmin Hong [a,1], Surendar Moogi [b], Krishna Pal Singh [c], Sanjay Kumar Arora [d], Vinod Kumar [e,f], Manisha Nanda [g], Anuj Kumar [h], Hyunook Kim [a,*]

[a] Water-Energy Nexus Laboratory, Department of Environmental Engineering, University of Seoul, Seoul 02504, Republic of Korea
[b] Biosystems Engineering Department, 200 Corley Building, Auburn University, Auburn, AL 36849, USA
[c] Department of Chemistry, DAV (PG) College Muzaffarnagar, 251001 Uttar Pradesh, India
[d] Department of Chemistry, SD College Muzaffarnagar, 251001 Uttar Pradesh, India
[e] Department of Food Science and Technology, Graphic Era (Deemed to be University), Dehradun, Uttarakhand 248002, India
[f] Peoples' Friendship University of Russia (RUDN University), 6 Miklukho-Maklaya Street, 117198 Moscow, Russian Federation
[g] Department of Microbiology, Graphic Era (Deemed to Be University), Dehradun, Uttarakhand 248002, India
[h] Department of Chemistry, School of Applied and Life Sciences (SALS), Uttaranchal University, Dehradun, Uttarakhand 248007, India

ARTICLE INFO

Editor: Dr Philiswa Nomngongo

Keywords:
PFAS rapid separation
β-cyclodextrin (β-CD) polymer
Multiple separation
Environmental relevant concentrations
Water treatment

ABSTRACT

Per- and polyfluorinated alkyl substances (PFASs), particularly long-chain compounds such as perfluorooctanoic acid (PFOA), perfluorooctanesulfonic acid (PFOS), perfluorononanoic acid (PFNA), and perfluorodecanoic acid (PFDA), are pervasive contaminants of global surface and groundwater resources. They have a significant negative impact on human health. Among the existing remediation techniques, adsorption remains an effective method and widely applied for removing PFASs from water. However, the limited adsorption kinetics of conventional adsorbents have motivated the development of advanced materials. In this study, we have synthesized a β-cyclodextrin (β-CD) polymer crosslinked with decafluorobiphenyl (β-CD–DFB) for the efficient separation of multiple long- and short-chain PFASs at environmentally relevant concentrations. The β-CD–DFB polymer exhibited a significant Langmuir adsorption capacity (43.10 ± 4.30 mg g^{-1}) and 10-times better affinity (K_L = 1.10 ± 0.40 L mg^{-1}) for long-chain PFOS compared to short-chain PFASs, with kinetics comparable to powdered activated carbons (ACs) and biochars (Act-BCs). Notably, the β-CD–DFB polymer could reduce the concentrations of long-chain PFASs in water from 1 to 44 ng L^{-1} via adsorption, significantly below the advisory level (i.e., 70 ng L^{-1}) set by the US Environmental Protection Agency and Korea Ministry of Environment. The adsorbent was easily regenerated simply by washing with methanol and maintained a high performance over five consecutive adsorption–desorption cycles. Furthermore, the performance of the adsorbent remained unaffected by natural organic matter (such as humic acid), which is a common AC foulant. Adsorption tests with real wastewater samples confirmed the potential of β-CD–DFB as a promising adsorbent for selective long-chain PFAS removal in water and wastewater treatment applications.

1. Introduction

Per- and polyfluoroalkyl substances (PFASs), particularly long-chain compounds such as perfluorooctanoic acid (PFOA) and perfluorooctanesulfonic acid (PFOS), contaminate surface and ground water if not effectively treated [1–3]. These compounds have been extensively used in various domestic and industrial applications, including aqueous film-forming foams (AFFFs), fluoropolymer synthesis (e.g., PTFE), and consumer products such as water-, grease-, and stain-repellent coatings. PFASs exhibit environmental persistence and bio-accumulation potential, thus leading to various negative health effects, including thyroid diseases, cancer, and liver damage [4–7]. They are

* Corresponding author.
E-mail address: h_kim@uos.ac.kr (H. Kim).
[1] These authors contributed equally to this work.

https://doi.org/10.1016/j.seppur.2025.134917
Received 18 June 2025; Received in revised form 18 August 2025; Accepted 26 August 2025
Available online 26 August 2025

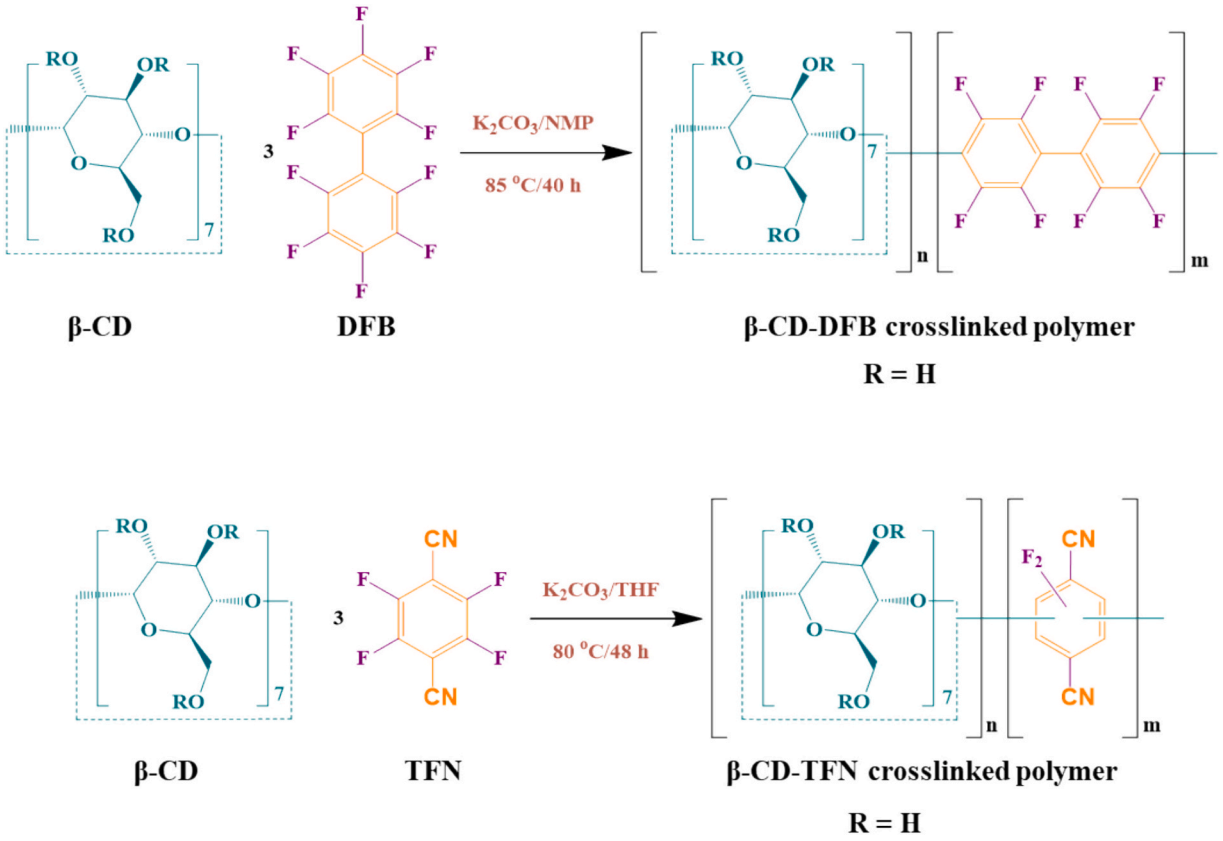

Scheme 1. Synthesis procedure for the β-cyclodextrin-crosslinked decafluorobiphenyl polymer (β-CD–DFB) adsorbent.

thermally and chemically stable against oxidation and resistant to hydrolysis, photolysis, and biodegradation because of their enormously high C–F dissociation energy (536 kJ mol^{-1}) [8]. Therefore, conventional degradation methods are often ineffective, and attempts at decomposition may produce toxic byproducts [9,10].

Adsorption is currently the only practical technique for removing organic pollutants (especially PFASs) from water resources because of its ease of design and operation, minimal sludge production, high efficiency, and repeatability [11–14]. A variety of adsorbents have been widely employed for this purpose, including granular or powdered activated carbons (GACs or PACs), carbon fibers [15,16], inorganic minerals [17], anionic exchange resins [18,19], metal–organic frameworks (MOFs) [20], and covalent organic frameworks (COFs) [21]. Among these, GAC is the most widely adopted adsorbent because of its cost-effectiveness and reasonable adsorption capacity particularly for long-chain PFASs. However, it suffers from slow kinetics, limited adsorption capacity, and poor affinity, particularly for short-chain PFASs, thus making it difficult to remove fluorinated compounds below regulatory standards [22]. In addition, it is easily fouled by dissolved natural organic matter (NOM) and inorganic constituents, and a significant amount of energy is required to regenerate PFAS-loaded GAC [23,24]. Therefore, the development of new adsorbents with rapid kinetics and good affinities is crucial for removing PFASs, particularly long-chain PFASs from water systems.

β-cyclodextrin (β-CD) crosslinked polymers are emerging adsorbents for the removal of organic pollutants like PFASs [4,25–29]. These β-CDs are inexpensive and commercially available cyclic oligosaccharides composed of seven glucose subunits and have non-covalent host–guest inclusion complexes resulting from their special toroid-shaped molecular structure (i.e., hydrophobic internal cavity and hydrophilic external surface) [30–32]. These crosslinked polymers have demonstrated rapid adsorption kinetics, high affinity, and significant potential for facile regeneration and reuse. For example, Errico et al. reported the association constants of $5.0 \pm 0.1 \times 10^5\ M^{-1}$ and $6.96 \pm 0.79 \times 10^5\ M^{-1}$ for the host–guest complexes of β-CD/PFOA and β-CD/PFOS, respectively [33]. Despite their high association constant values, some β-CD-based polymers, such as the tetrafluoroterephthalonitrile crosslinked β-CD (β-CD–TFN), demonstrate poor effectiveness in removing long- and short-chain PFASs, even though they have been known to efficiently remove other organic contaminants [4,34,35]. These mesoporous β-CD-polymeric-network-based adsorbents with high surface areas were synthesized via nucleophilic aromatic substitution reactions between unmodified β-CD and rigid aromatic crosslinkers [35,36]. It has also been reported that variations in crosslinker chemistry affect the kinetics, adsorption capacity, and selectivity of polymers in adsorbing PFASs [4,36]. Xiao et al. reported that the decafluorobiphenyl crosslinked β-CD polymer (β-CD–DFB) could reduce the concentration of PFOA in water from 1 to < 10 ng L^{-1}, while resisting humic acid fouling and enabling methanol-assisted regeneration [25]. Recently, Chaudhary et al. reported a dual adsorption mechanism of β-CD–DFB for NH_4^+-PFOA, involving both electrostatic and hydrophobic interactions [37]. This adsorbent was designed to form stable host–guest inclusion complexes between β-CD and PFOA via secondary non-covalent interactions with crosslinkers. Nevertheless, a systematic evaluation under different water treatment conditions, including pH, kinetics, and electron affinity, for both long- and short-chain PFASs has not yet been performed.

Here, we employed a β-CD–DFB polymer, derived from the crosslinking of DFB and β-CD via a nucleophilic aromatic substitution reaction, to investigate—for the first time—the effects of various parameters on the removal of 10 model PFASs at 1 μg L^{-1} each. Its performance was compared with those of β-CD–TFN and activated biochar (Act-BC). The adsorption efficiency was systematically evaluated under different water treatment conditions, including pH, kinetics, and initial PFAS concentrations. Additionally, we have evaluated the regeneration and reusability of β-CD–DFB via multiple adsorption–desorption cycles and investigated its performance in the presence of NOM and real

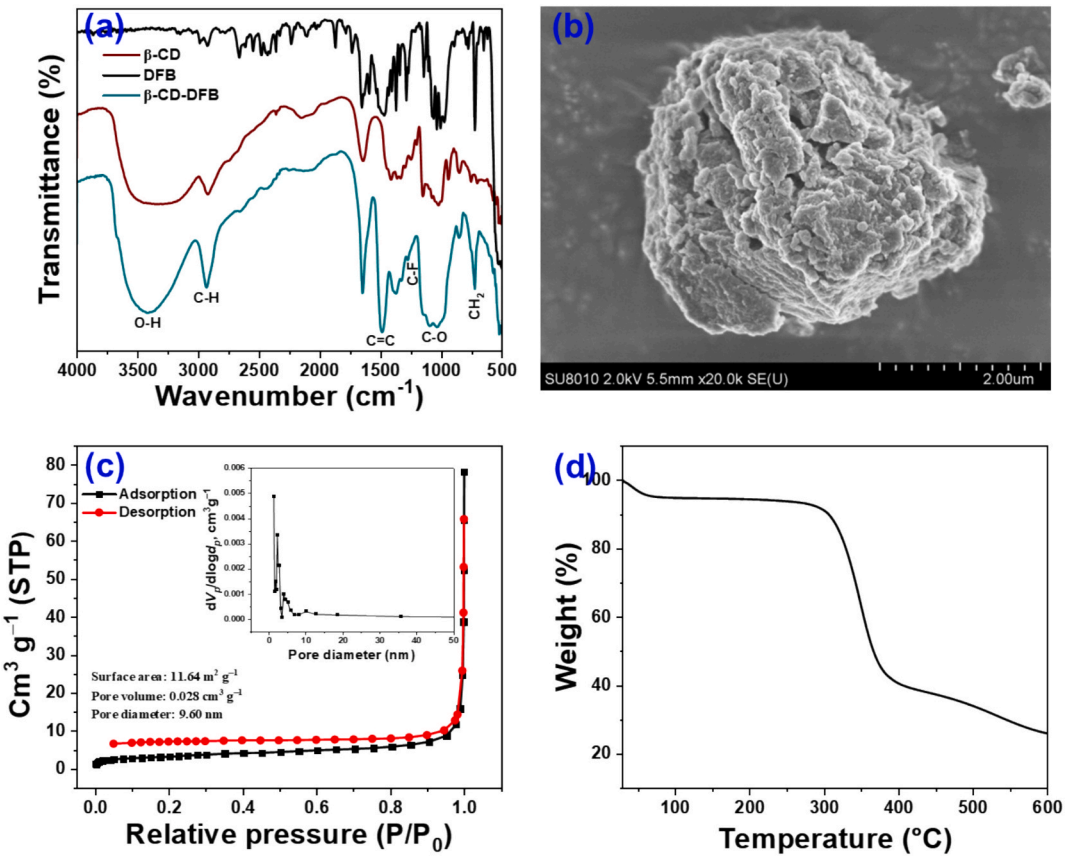

Fig. 1. FTIR spectra (a), FESEM image (b), N_2 adsorption–desorption and pore size distribution (inset) (c), and TGA (d) of β-CD–DFB.

wastewater (WW) matrices. Lastly, this study for the first time highlights the selective affinity of β-CD–DFB adsorbent for long-chain PFASs, thus demonstrating its potential as a tunable adsorbent for targeted PFAS removal in water treatment applications.

2. Materials and methods

2.1. Chemicals and reagents

All the chemicals, including the targeted PFASs, were obtained from commercial suppliers (WENi, Seoul, South Korea) and used as received. Detailed information is provided in Supporting Information (Text SI-1A).

2.2. Procedure for the synthesis of β-CD–DFB polymer

The crosslinked polymer network β-CD–DFB was synthesized via nucleophilic aromatic substitution between β-CD and DFB. A detailed synthesis procedure is provided in Text SI-1B, and the reaction scheme is illustrated in Scheme 1.

2.3. Characterization of β-CD–DFB

Quantification of PFOS (10–200 ng L^{-1}) in aqueous solutions was performed using ultra-high-performance liquid chromatography tandem mass spectrometry (LC-MS/MS) with electrospray ionization (LCMS-8050^{TM}, Shimadzu, Kyoto, Japan). The mobile phase used for separating PFASs of 1 μg L^{-1} consisted of (A) 20 mM ammonium acetate (Sigma-Aldrich, St. Louis, MO, USA; prepared in Milli-Q water) and (B) 75 % acetonitrile (HPLC-grade; Sigma-Aldrich, St. Louis, MO, USA) (acetonitrile:water (75:25). A detailed discussion of the quantification methods for the target PFASs and the characterization techniques are presented in Text SI-2.

2.4. Batch adsorption experiments

Different batch adsorption experiments were conducted in the polypropylene scintillation vials at 24 ± 1 °C using a multi-position incubator (DAIHAN Scientific, Seoul, South Korea) with a shaking rate of 200 rpm to evaluate the adsorption performance of β-CD–DFB toward PFASs. Details of all the experimental parameters, including pH, kinetics, isotherms, regeneration, and stability, are provided in Text SI-3.

3. Results and discussion

3.1. Characterization of β-CD–DFB

For confirming the synthesis of β-CD–DFB, Fourier transform infrared spectroscopy (FTIR) analysis was performed with the polymeric material and the results are presented in Fig. 1(a). The characteristic peaks were observed at 3411, 2934, 1033, and 726 cm^{-1} which are corresponding to O–H stretching, aliphatic C–H stretching, C–O stretching, and CH_2 rocking vibrations of β-CD in the β-CD–DFB polymer. After reaction, the spectrum showed a new peak at 1492 cm^{-1}, which corresponds to aromatic C=C, confirming the successful formation of β-CD–DFB [38]. All the FTIR major peaks of β-CD–DFB are shown in Table SI-2.

In support of β-CD–DFB synthesis, X-ray photoelectron spectroscopy (XPS) was applied for the material, and its full scan spectra for β-CD–DFB before and after PFOS adsorption are presented in Fig. SI-1. Before adsorption, β-CD–DFB showed three binding energy peaks at 286.5, 532.5, and 688.5 eV, which correspond to C 1s, O 1s, and F 1s, respectively, confirming the crosslinking between β-CD and DFB. The surface morphology of β-CD–DFB was examined using field-emission scanning

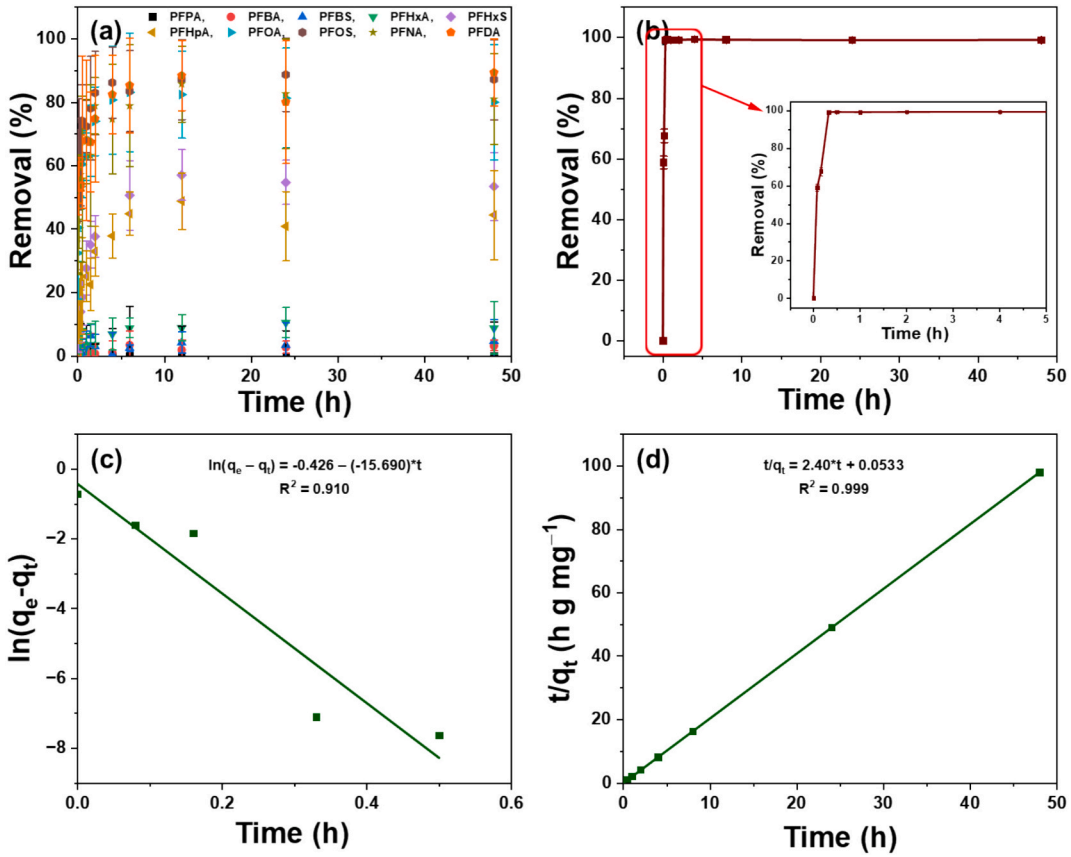

Fig. 2. Kinetics of 10 PFASs adsorption (concentration of each PFAS = 1 μg L^{-1}, adsorbent dose = 10 mg L^{-1}, pH 5.0) (a) and PFOS adsorption ($[PFOS]_0$ = 200 μg L^{-1}, adsorbent dose = 400 mg L^{-1}) onto β-CD–DFB (b). Linear fitting of PFO (c) and PSO (d) kinetics.

Table 1
PFO and PSO linear kinetics fitting results for adsorption of PFOS onto β-CD–DFB polymer.

Models	Parameters	PFOS
PFO	$q_{e,exp}$ (mg g^{-1})	0.50
	$q_{e,cal}$ (mg g^{-1})	2.68
	k_1 (h^{-1})	15.70
	R^2	0.910
PSO	$q_{e,cal}$ (mg g^{-1})	0.490
	k_2 (g $mg^{-1}h^{-1}$)	78.10
	R^2	0.999

electron microscopy (FESEM) at lower and higher magnifications (Fig. 1 (b) and Fig. SI-2, respectively), indicating a slightly spherical rigid structure. This rigid type of structure confirmed the better stability of β-CD–DFB. The EDS-based elemental mapping (Fig. SI-3(a)–(d)) demonstrated a uniform distribution of C, O, and F across the surface. Quantitative energy dispersive X-ray spectrometer (EDS) analysis (Fig. SI-3(e)–(f)) further confirmed the atomic composition of 82.4 % C, 11.5 % O, and 6.1 % F, which was consistent with the expected structure with the F element inserted. The Brunauer–Emmett–Teller (BET) surface area, pore volume, and pore diameter of β-CD–DFB were determined using the N_2 adsorption–desorption isotherm (Fig. 1(c)), and were found to be 11.64 m^2 g^{-1}, 0.028 cm^3 g^{-1}, and 9.60 nm, respectively. This surface area is not sufficient for adsorbing a large amount of PFAS because the adsorption to β-CD–DFB primarily depends on the availability of hydrophobic sites in the form of β-CD's cavity. The pore size distribution (inset of Fig. 1(c)) further confirms its nonporous structure, which is consistent with the FESEM morphology. Notably, this surface area and porosity are completely opposite to those of β-CD–TFN, possibly due to the rigid biphenyl core, which introduces steric

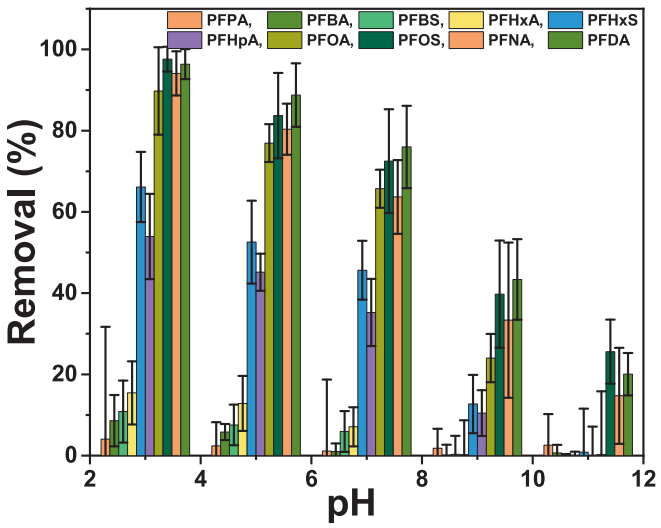

Fig. 3. Ph effect on removal efficiencies of β-cd–dfb for 10 pfass ($[pfass]_0$ = 1 μg L^{-1}, adsorbent dose = 10 mg L^{-1}, pH range = 3–11). Error bars indicate the standard deviation.

hindrance to inhibit the formation of porous adsorbent [4]. The thermal stability of β-CD–DFB was evaluated using thermogravimetric analysis (TGA) (Fig. 1(d)). Initially, a small weight loss of 5.40 % was observed between 30 and 80 °C, attributed to moisture evaporation. Between 80 and 280 °C, the mass of polymer remained relatively stable, suggesting the completion of water crystallization or evaporation. In the next stage, a significant weight loss (i.e., 52 %) was observed between 260 and

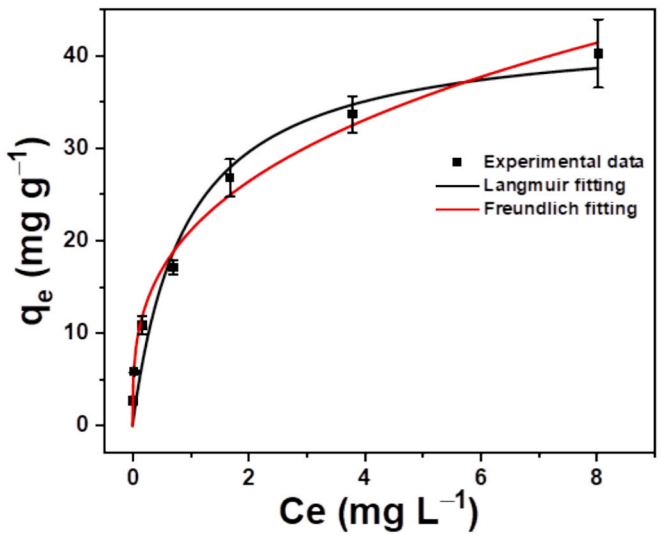

Fig. 4. Nonlinear isotherms of PFOS adsorption onto β-CD–DFB ($[PFOS]_0$ range = 0.05–15 mg L^{-1}, adsorbent dose = 200 mg L^{-1}, pH 3.0). Error bars indicate the standard deviation.

Table 2
Nonlinear isotherm fitting parameters for the PFOS adsorption onto the β-CD–DFB polymer.

Models	Parameters	PFOS
Langmuir	$q_{m,exp}$ (mg g^{-1})	40.30 ± 3.70
	$q_{m,cal}$ (mg g^{-1})	43.10 ± 4.30
	K_L (L mg^{-1})	1.10 ± 0.40
	R^2	0.951
Freundlich	K_F (mg g^{-1}) (L mg^{-1})$^{1/n}$	21.10 ± 0.90
	n	3.10 ± 0.20
	R^2	0.986

400 °C, most likely due to the thermal decomposition of β-CD and DFB moieties. A gradual mass loss was observed above 400 °C, possibly owing to the breakdown of the carbon framework [39].

3.2. Adsorption kinetics

The adsorption performance of β-CD–DFB was evaluated for the removal of 10 targeted PFASs from water, including seven perfluoroalkyl carboxylic acids (PFCAs) with C-numbers of 3, 4, 6, 7, 8, 9, and 10 and three perfluoroalkyl sulfonates (PFSAs) with C-numbers of 4, 6, and 8 (Text SI-1A). The experiment was conducted using a PFAS mixture (1 μg L^{-1} each) at pH 5.0 and β-CD–DFB (10 mg L^{-1}). The results, as presented in Fig. 2(a) and Fig. SI-4, clearly show that the PFASs rapidly occupied the adsorption sites on β-CD–DFB and reached equilibrium in 12 h. The removal efficiencies were found to be greater than 83 % for long-chain PFASs (PFOA, PFOS, PFNA, and PFDA) and less than 57 % for short-chain ones (i.e., PFPA, PBBA, PFBS, PFHxA, PFHpA, and PFHxS). The greater adsorption efficiencies observed for long-chain PFASs were attributed to their strong hydrophobic interaction with the cavity of β-CD. For PFPA, PFBA, and PFBS, extremely low removal efficiencies (less than 8 %) were obtained, which was attributed to their low hydrophobic interactions with the cavity of β-CD. Previously, Murai

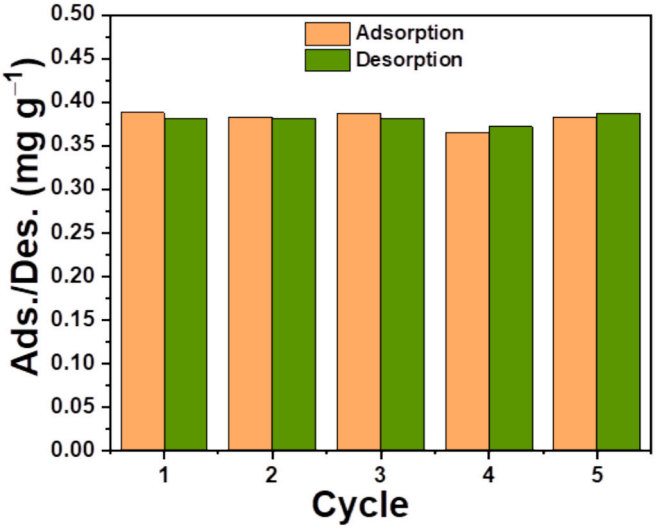

Fig. 6. Adsorption–desorption capacity during regeneration and reuse of the β-CD–DFB polymer by simple washing with methanol. For adsorption: $[PFOS]_0$ = 200 μg L^{-1}, adsorbent dose = 500 mg L^{-1}. For desorption: β-CD–DFB polymer was suspended in 50 mL methanol for 24 h.

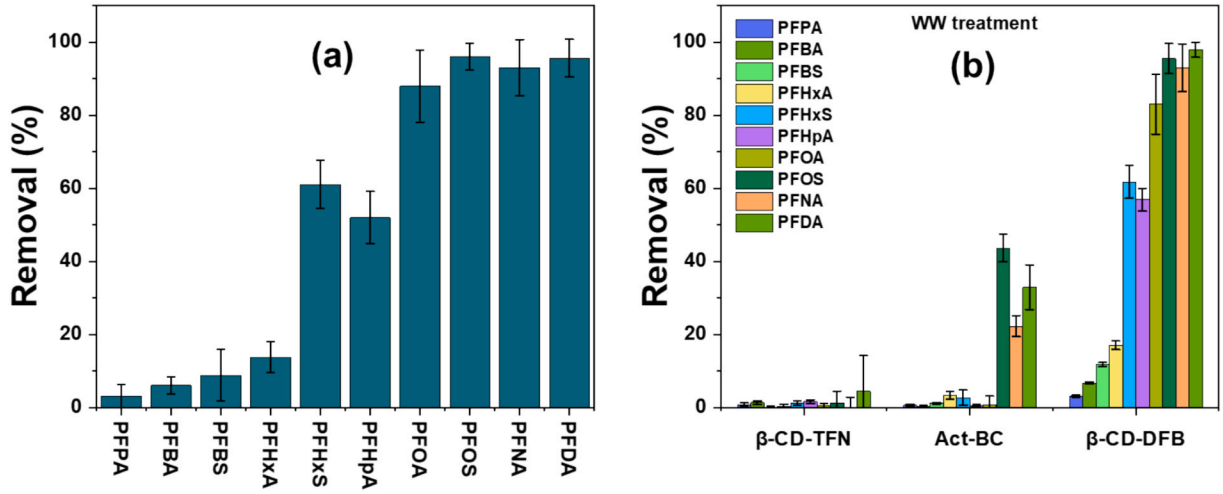

Fig. 5. Effect of humic acid (20 mg L^{-1}) on percent removal adsorption of β-CD–DFB for 10 PFASs (a), and percent removal efficiencies of β-CD–TFN, Act-BC, and β-CD–DFB for 10 PFASs in real filtered WW (b) (initial concentration of each PFASs = 1 μg L^{-1}, doses of adsorbents = 10 mg L^{-1} each, pH 3.0). Error bars indicate the standard deviation.

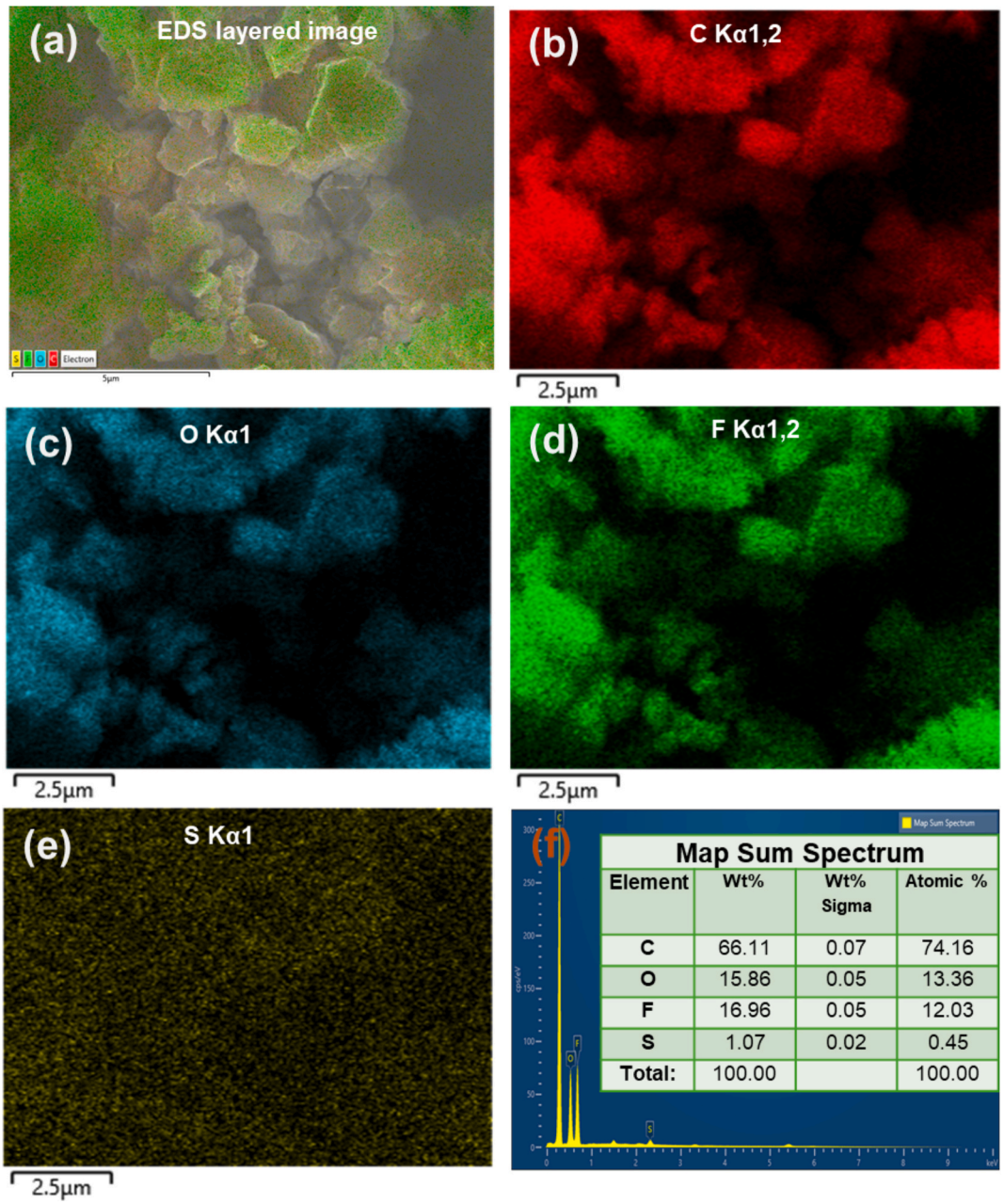

Fig. 7. EDS mapping of β-CD–DFB polymer after PFOS adsorption; EDS layered image (a), C Ka1,2 mapping (b), O Ka1 mapping (c), F Ka1,2 mapping (d), S Ka1 mapping (e), and EDS spectra (f) and elemental composition in inset of (f).

et al. reported that the long-chain PFASs were more readily adsorbed by β-CD-based polymeric adsorbent than short-chain PFASs [40]. They also reported that the β-CD would have the tendency to form host–guest inclusion complexes with PFAS molecules and the stability constant of these complexes increase with chain length as long-chain PFASs exhibit greater hydrophobicity than the shorter C-chain PFASs. The high hydrophobicity of long-chain PFASs allows molecules to migrate from the aqueous phase to the adsorbent surface. Considering that the cavities of β-CD in β-CD–DFB would serve as adsorption sites for PFASs, the long-chain PFASs interacted strongly with these cavities relative to interior pores of β-CD–DFB due to their better fitting, resulting in higher removal efficiencies [27]. Notably, the adsorbent demonstrated higher adsorption for PFSAs than PFCAs of the equivalent carbon chain length and were found to have a better removal efficiency with PFSAs. This selectivity of β-CD–DFB was attributed to the presence of a sulfonate head group in PFSAs. This electron rich group suggested that the β-CD would have the tendency to capture long-chain PFASs into its cavity in a complementary manner [27]. These findings were consistent with the adsorption affinities observed for GAC, resins, and other reported adsorption materials for PFASs [18]. However, β-CD–DFB showed negligible removal efficiencies (< 8 %) for short-chain PFASs (i.e., PFPA, PFBA, and PFBS), which is almost 14 magnitudes smaller than the long-chain PFASs, as their small size and low hydrophobicity hinder effective cavity complexation.

The adsorption kinetics of PFASs onto β-CD–DFB was evaluated by performing adsorption experiments with PFOS as a model compound (initial concentration = 200 µg L^{-1}, pH, 3.0, and adsorbent dose = 400 mg L^{-1}). As shown in Fig. 2(b), a high removal efficiency (> 99 %) was achieved only within the first 20 min of contact time. This result can be attributed to the strong hydrophobic interactions between PFOS and the cavity of β-CD, facilitating immediate formation of host–guest inclusion complexes [28,29,41].

Two well-known kinetic models, i.e., pseudo-first-order (PFO) [42] and pseudo-second-order (PSO) [43], were applied to the kinetic data (Fig. 2(c) and (d)), and the results are presented in Table 1. The adsorption data showed significantly better agreement with the PSO model ($R^2 = 0.999$) than with the PFO model ($R^2 = 0.910$), indicating the chemisorption process. The calculated rate constant (k_2) value was found to be 78.10 g $mg^{-1}h^{-1}$, indicating a rapid adsorption kinetics to attain the equilibrium. Notably, this k_2 value was significantly higher than those reported for conventional adsorbents including GAC and PAC, highlighting the superior kinetic performance of β-CD–DFB (Table SI-3).

3.3. pH effect

The solution pH significantly affects the PFAS adsorption by β-CD–DFB. Therefore, the pH effect on the adsorption of target PFASs on β-CD–DFB was evaluated, and the results are presented in Fig. 3. The removal efficiencies of β-CD–DFB for PFASs decreased as the pH increased. The removal efficiencies of PFHxS, PFHpA, PFOA, PFOS, PFNA, and PFDA, respectively were 66.1 %, 53.1 %, 89.8 %, 97.6 %, 94.1 %, and 96.4 %, respectively, at pH 3.0. However, they decreased to 45.60 %, 35.20 %, 65.70 %, 72.50 %, 63.70 %, and 75.10 %, respectively, at pH 7.0. Under the experimental conditions, the used PFASs existed in anionic or less positive forms (Table SI-1) and the calculated zeta potential was less negative (-1.2 ± 0.61) at pH 3.0 than at pH 5.0 (-7.2 ± 0.37). This suggests that the removal efficiencies of the adsorbent for most PFASs would be higher at pH 3.0 compared to those at higher pHs. From the data, it is clearly observed that although the pK_a values of long-chain PFASs such as PFHxS, PFOA, PFOS, PFNA and PFDA were not supportive of interactions with β-CD–DFB, still better removal efficiencies could be obtained. For example, the pKa value of PFOA is −0.2, whereas that of PFOS is highly negative (−3.27), meaning that PFOS creates more electrostatic repulsion than PFOA. Nevertheless, a better removal efficiency was obtained for PFOS. This is possibly due to more opportunities for adsorption via hydrophobic interactions (host–guest inclusion formation), as more negative charges result in more hydrophobic interactions [27].

The adsorption equilibrium of the synthesized material for the 10 target PFASs was also evaluated at pH 3.0 to obtain similar results to those obtained in the experiment evaluating the effect of pH, suggesting better adsorption efficiencies for long-chain PFASs than those for short-chain PFASs (Fig. SI-5).

3.4. Adsorption isotherm

As shown in the kinetics and pH-dependent adsorption studies, the superior removal efficiencies of β-CD–DFB for long-chain PFASs were most likely due to the host–guest binding sites of β-CD within β-CD–DFB polymer. Therefore, the adsorption capacity and affinity of β-CD–DFB for PFOS were evaluated by performing isotherm experiments. The initial PFOS concentration was varied from 0.5 to 15 mg L^{-1} at pH 3.0 with adsorbent dose of 200 mg L^{-1} and equilibrium time of 16 h.

Langmuir and Freundlich isotherm models were applied for fitting the PFOS isotherm data (Fig. 4), and the results are listed in Table 2. The Langmuir isotherm fit shows that the adsorption capacity of β-CD–DFB was 43.1 ± 4.3 mg L^{-1}, which is comparable with those of other adsorbents including GAC, AC, and MOFs [44]. The calculated Langmuir affinity coefficient of the adsorbent for PFOS ($K_L = 1.10$ L mg^{-1}) was approximately 10 times higher than those of AC (approximately 0.1 L mg^{-1}) [22] and anion exchange resin (approximately 0.1 L mg^{-1}) [22], but smaller than that of chitosan beads (22.8 L mg^{-1}) [45], which confirmed the superior affinity of β-CD–DFB for long-chain PFASs. While both Langmuir and Freundlich exhibited good fits to the PFOS isotherms data (Table 2), the Freundlich isotherm better described the adsorption equilibrium behavior of PFOS on β-CD–DFB. This was probably due to unsaturation behavior within the used concentration range; therefore, the calculated adsorption capacity of the β-CD–DFB should be considered as conservative.

3.5. Effect of NOM

The performance of AC is highly affected by fouling in the presence of other organic co-contaminants and NOM, whereas β-CD-based polymeric adsorbents are known to some degree resistant to fouling [37]. To evaluate this effect, the influence of humic acid (20 mg L^{-1}), an important component of NOM, on the adsorption of PFASs by β-CD–DFB (10 mg L^{-1}) was evaluated at environmentally relevant concentrations (1 μg L^{-1} each). As shown in Fig. 5(a), presence of the humic acid did not significantly affect PFAS removal by β-CD–DFB; over 87 % adsorption efficiency was maintained for long-chain PFOA, PFOS, PFNA, and PFDA. These results further confirm the superior fouling resistance and strong affinity of β-CD–DFB for long-chain PFASs.

3.6. PFAS adsorption in WW matrix

Generally, PFASs exist in water containing other organic pollutants, which restrict the efficiency of an adsorbent owing to its lower selectivity. As discussed in the kinetics section, β-CD–DFB showed a high removal efficiency for long-chain PFASs in pure water (i.e., > 83 %); therefore, the performance of β-CD–DFB was evaluated for PFASs in real WW matrix and compared with those of Act-BC (PAC) and β-CD–TFN on an equivalent mass basis (Fig. 5(b)). The WW used in these experiments was collected from a local WW treatment plant in Seoul, Korea, which was free of detectable levels of all the PFASs used in this study and had a pH of 12.6. The pH was adjusted to approximately 3.1 based on the results of the experiment for pH effect, and the stock solution with 10 PFASs was diluted to generate an initial concentration of 1 μg L^{-1} for each compound. The dose of adsorbents evaluated in this experiment was 10 mg L^{-1}, and the equilibrium time was 16 h.

As presented in Fig. 5(b), Act-BC clearly showed poor removal efficiencies (< 44 %) for all the target PFASs, while its surface area (47.46 m^2 g^{-1}) was quite high, compared to β-CD–DFB which showed more than 95 % removal efficiencies [34,46]. The lower adsorption efficiency of Act-BC for PFASs was attributed to the lack of active functional groups and porosity suitable for capturing PFASs in a stable form. In Table SI-3, the absorption capacity and kinetic affinity of β-CD–DFB are compared with those of other reported adsorbents, highlighting anomalously higher values for GAC and PAC. This observation is attributed to their large surface area and suitable porosity, which facilitate micelle formation via hydrophobic interaction during the adsorption of PFASs [47]. Overall, the adsorption capacity of β-CD–DFB for PFASs was comparable to those of leading PACs, and therefore demonstrated superior performance compared to GACs (Table SI-3). Based on the equilibrium removal efficiencies of β-CD–TFN for the 10 PFASs, the adsorbent was found to have an extremely poor affinity for both short- and long-chain PFASs (approximately 3 % PFASs) although it is known to have a large surface area (263 m^2 g^{-1}) and high adsorption capacities for many organic micropollutants [35].

In the case of β-CD–DFB, the remaining concentration of long-chain PFASs was lower than 44 ng L^{-1} after treatment with β-CD–DFB, which is significantly lower than the established health advisory level set by the Ministry of Environmental, South Korea (70 ng L^{-1}) [48]. Additionally, the adsorption efficiency of β-CD–DFB was not found to be greatly affected by other WW constituents, suggesting that the β-CD–DFB polymer would be a promising adsorbent for effectively treating WW contaminated by long-chain PFASs at environmental relevant concentrations.

3.7. β-CD–DFB regeneration and reuse

For the effective and economical removal of PFASs from WW, regeneration and reusability are also crucial factors for practical

application of β-CD–DFB. Therefore, five consecutive cycles of adsorption and desorption were performed with PFOS-loaded β-CD–DFB (initial PFOS concentration = 200 μg L^{-1}, adsorbent dose = 500 mg L^{-1}, pH 5.0), and the results are presented in Fig. 6. The adsorption was carried out with 50-mg β-CD–DFB in 100-mL PFOS solution for 16 h, whereas desorption was carried out by suspending the PFOS-loaded adsorbent into 50 mL methanol for 24 h. The results indicated that the amounts of adsorbed and desorbed PFOS were almost equal, even after five consecutive cycles of adsorption and desorption, without any significant loss in adsorption capacity. In an additional experiment, it was found that the complete desorption of PFOS from β-CD–DFB could be achieved within 10 min, thus demonstrating the potential for rapid and efficient regeneration; regeneration of GAC and PAC after their adsorption of PFASs requires a relatively long regeneration time [49]. These results underscore the potential of β-CD–DFB as a reusable, efficient, and economically viable adsorbent for PFAS removal in real-world applications.

3.8. Adsorption mechanism

From the above discussion, the higher affinity of β-CD–DFB for long-chain PFASs can be attributed to the interactions between PFAS molecules and the cavities of β-CD. Each of adsorbed long-chain PFASs consists of a sulphonic or carboxylic head and a carbon chain with C–F bond, while β-CD possesses hollow hydrophobic inner cavities of suitable size and structure that tightly can adsorb long-chain PFAS molecules by forming host–guest complexes [29]. Elemental mapping, compositional analysis (EDS), XPS, and FTIR techniques were performed before and after PFOS adsorption by β-CD–DFB to examine the adsorption mechanism between the polymeric adsorbent and PFASs. The EDS analysis performed after the PFOS adsorption confirmed the uniform distribution of elements (i.e., C, O, and F) throughout the whole surface along with the insertion of sulfur in the form of PFOS (Fig. 7), confirming the adsorption of PFOS on the surface of β-CD–DFB. The atomic percentages of C, O, F, and S were 74.2 %, 13.4 %, 12.0 %, and 0.45 %, respectively. The full-scan XPS spectrum obtained for β-CD–DFB after the adsorption of PFOS showed an additional peak of S 2p (from SO_3^- group of PFOS) at 168.5 eV, without any significant change in other C 1S, O 1S, and F 1S binding energy peaks, confirming the adsorption of PFOS via only the host–guest inclusion complex formation (hydrophobic interaction). To support the XPS result, FTIR spectra were also obtained (Fig. SI-6); although the peak positions for all the elements were not changed after PFOS adsorption, a new peak was observed for S=O at 1244 cm^{-1}, indicating the hydrophobic interaction of PFOS with the cavities of β-CD–DFB. Previously, NMR measurements and simulation data also confirmed the adsorption of PFOA onto β-CD polymer through the insertion of the fluorinated tail of PFOA inside the hydrophobic interstitial cavities of β-CD [37,50]. Xiao et al. reported a similar type hydrophobic interaction between the PFOA and β-CD molecules [4]. The β-CD cavity is electron-deficient while the entire PFOS molecule, particularly its sulfonate head, is electron-rich, suggesting a favorable adsorption between the β-CD cavity and PFOS. Weiss-Errico et al. also reported a similar type of the host–guest interaction between β-CD's cavity and PFASs using ^{19}F NMR characterization [51].

4. Conclusion

In summary, β-CD–DFB, a crosslinked polymer, was prepared using the nucleophilic aromatic substitution reaction and characterized using different techniques. The kinetics results showed faster adsorption for longer-chain PFASs than for shorter-chain PFASs, with removal efficiencies of more than 83 %. The adsorbent reduces the long-chain PFAS concentration to less than 44 ng L^{-1}, which is much lower than the water quality standard set by the Ministry of Environment, South Korea (70 ng L^{-1}). The rate constant k_2 was sufficiently high enough (78.10 g $mg^{-1}h^{-1}$) to lead ultra-rapid adsorption to attain equilibrium. The adsorption capacity and affinity coefficient of β-CD–DFB calculated by the Langmuir isotherm fit were 43.10 ± 4.30 mg L^{-1} and 1.10 mg^{-1}, respectively. This adsorption capacity is in the range of those of GAC and other reported adsorbents, whereas the affinity is more than 10 times better than those calculated for GAC and PAC. pH data confirmed the highest removal efficiency for the majority of PFASs at pH 3.0, which suggests that not only surface charge but also other key factors affect the affinity of β-CD–DFB polymer in PFAS adsorption. Experiments conducted with samples with NOM and with WW matrices confirmed that the presence of other constituents did not affect the adsorption efficiencies of the adsorbent. Notably, the current adsorbent reduces the long-chain PFAS concentration to less than 44 ng L^{-1}, which is lower than that set by the Ministry of Environment, South Korea (70 ng L^{-1}). Finally, the adsorbent was easily regenerated by methanol washing without any loss of efficiency. The adsorption mechanism confirmed the crucial role of hydrophobic interactions in PFAS removal; these characteristics make β-CD–DFB an emerging candidate for the removal of long-chain PFOSs. Further studies will aim to modify β-CD with an amine-functionalized tripodal crosslinker for the effective removal of short-chain PFASs along with long-chain PFASs.

CRediT authorship contribution statement

Monu Verma: Writing – original draft, Investigation, Funding acquisition, Formal analysis, Data curation, Conceptualization. **Youngmin Hong:** Investigation. **Surendar Moogi:** Software. **Krishna Pal Singh:** Software. **Sanjay Kumar Arora:** Software. **Vinod Kumar:** Visualization. **Manisha Nanda:** Validation. **Anuj Kumar:** Software. **Hyunook Kim:** Writing – review & editing.

Declaration of competing interest

The authors declare that they have no known competing financial interests or personal relationships that could have appeared to influence the work reported in this paper.

Acknowledgements

Monu Verma would like to thank the National Research Foundation of Korea (NRF) for funding provided by the Ministry of Science and ICT through the Brain Pool Program (RS-2024-00406513). H. Kim was supported by the Korean Ministry of Environment (MOE) through a grant for the development of innovative drinking water and wastewater technologies (2019002710006) and Special Graduate Program for Post-plastics Era supported by the Korea Environmental Industry and Technology Institute. This work was supported by the RUDN University Strategic Academic Leadership Program.

Appendix A. Supplementary data

Supplementary data to this article can be found online at https://doi.org/10.1016/j.seppur.2025.134917.

Data availability

Data will be made available on request.

References

[1] J. He, A. Gomeniuc, Y. Olshansky, J. Hatton, L. Abrell, J.A. Field, J. Chorover, R. Sierra-Alvarez, Enhanced removal of per- and polyfluoroalkyl substances by crosslinked polyaniline polymers, Chem. Eng. J. 446 (2022) 137246, https://doi.org/10.1016/j.cej.2022.137246.

[2] E. Gagliano, M. Sgroi, P.P. Falciglia, F.G.A. Vagliasindi, P. Roccaro, Removal of poly- and perfluoroalkyl substances (PFAS) from water by adsorption: Role of PFAS chain length, effect of organic matter and challenges in adsorbent regeneration, Water Res. 171 (2020) 115381, https://doi.org/10.1016/j.watres.2019.115381.

[3] Y. He, J. Zhou, Y. Li, Y.D. Yang, J.L. Sessler, X. Chi, Fluorinated nonporous adaptive cages for the efficient removal of perfluorooctanoic acid from aqueous source phases, J. Am. Chem. Soc. 146 (2024) 6225–6230, https://doi.org/10.1021/jacs.3c14213.

[4] L. Xiao, Y. Ling, A. Alsbaiee, C. Li, D.E. Helbling, W.R. Dichtel, β-Cyclodextrin polymer network sequesters perfluorooctanoic acid at environmentally relevant concentrations, J. Am. Chem. Soc. 139 (2017) 7689–7692, https://doi.org/10.1021/jacs.7b02381.

[5] S.C.E. Leung, D. Wanninayake, D. Chen, N.T. Nguyen, Q. Li, Physicochemical properties and interactions of perfluoroalkyl substances (PFAS) - challenges and opportunities in sensing and remediation, Sci. Total Environ. 905 (2023) 166764, https://doi.org/10.1016/j.scitotenv.2023.166764.

[6] P. Exposure, V. Gallo, G. Leonardi, B. Genser, S.J. Frisbee, Concentrations and Liver Function Biomarkers in a Population with Elevated, Environ. Health Perspect. 120 (2012) 655–660.

[7] S.P. Lenka, M. Kah, L.P. Padhye, A review of the occurrence, transformation, and removal of poly- and perfluoroalkyl substances (PFAS) in wastewater treatment plants, Water Res. 199 (2021) 117187, https://doi.org/10.1016/j.watres.2021.117187.

[8] F. Li, J. Duan, S. Tian, H. Ji, Y. Zhu, Z. Wei, D. Zhao, Short-chain per- and polyfluoroalkyl substances in aquatic systems: Occurrence, impacts and treatment, Chem. Eng. J. 380 (2020) 122506, https://doi.org/10.1016/J.CEJ.2019.122506.

[9] H. Moriwaki, Y. Takagi, M. Tanaka, K. Tsuruho, K. Okitsu, Y. Maeda, Sonochemical decomposition of perfluorooctane sulfonate and perfluorooctanoic acid, Environ. Sci. Technol. 39 (2005) 3388–3392, https://doi.org/10.1021/es040342v.

[10] H. Hori, E. Hayakawa, H. Einaga, S. Kutsuna, K. Koike, T. Ibusuki, H. Kiatagawa, R. Arakawa, Decomposition of environmentally persistent perfluorooctanoic acid in water by photochemical approaches, Environ. Sci. Technol. 38 (2004) 6118–6124, https://doi.org/10.1021/es049719n.

[11] M. Verma, I. Lee, V. Kumar, S. Yuan, P. Chihhao, F. Hyunook, Chitosan cross-linked β–cyclodextrin polymeric adsorbent for the removal of perfluorobutanesulfonate from aqueous solution: adsorption kinetics, isotherm, and mechanism, Environ. Sci. Pollut. Res. 30 (2023) 19259–19268, https://doi.org/10.1007/s11356-022-23546-z.

[12] X. Nie, G. Li, S. Li, Y. Luo, W. Luo, Q. Wan, T. An, Highly efficient adsorption and catalytic degradation of ciprofloxacin by a novel heterogeneous Fenton catalyst of hexapod-like pyrite nanosheets mineral clusters, Appl. Catal. B Environ. 300 (2022) 120734, https://doi.org/10.1016/j.apcatb.2021.120734.

[13] M. Verma, I. Tyagi, V. Kumar, S. Goel, D. Vaya, H. Kim, Fabrication of GO–MnO2 nanocomposite using hydrothermal process for cationic and anionic dyes adsorption: Kinetics, isotherm, and reusability, J. Environ. Chem. Eng. 9 (2021) 106045, https://doi.org/10.1016/j.jece.2021.106045.

[14] M. Verma, A. Kumar, I. Lee, V. Kumar, J.-H. Park, H. Kim, Simultaneous capturing of mixed contaminants from wastewater using novel one-pot chitosan functionalized with EDTA and graphene oxide adsorbent, Environ. Pollut. 304 (2022) 119130, https://doi.org/10.1016/j.envpol.2022.119130.

[15] B. Newman, E.H. Doeven, P.S. Francis, F. Stojcevski, D.J. Hayne, J.M. Chalker, L. C. Henderson, A high value application of reclaimed carbon fibers: Environmental remediation and redeployment in structural composites, Sustain. Mater. Technol. 35 (2023) e00546, https://doi.org/10.1016/j.susmat.2022.e00546.

[16] P.S. Pauletto, T.J. Bandosz, Activated carbon versus metal-organic frameworks: a review of their PFAS adsorption performance, J. Hazard. Mater. 425 (2022) 127810, https://doi.org/10.1016/j.jhazmat.2021.127810.

[17] S. Verma, R.S. Varma, M.N. Nadagouda, Remediation and mineralization processes for per- and polyfluoroalkyl substances (PFAS) in water: a review, Sci. Total Environ. 794 (2021) 148987, https://doi.org/10.1016/j.scitotenv.2021.148987.

[18] P. McCleaf, S. Englund, A. Östlund, K. Lindegren, K. Wiberg, L. Ahrens, Removal efficiency of multiple poly- and perfluoroalkyl substances (PFASs) in drinking water using granular activated carbon (GAC) and anion exchange (AE) column tests, Water Res. 120 (2017) 77–87, https://doi.org/10.1016/j.watres.2017.04.057.

[19] Y. Fang, A. Ellis, Y.J. Choi, T.H. Boyer, C.P. Higgins, C.E. Schaefer, T. J. Strathmann, Removal of per- and polyfluoroalkyl substances (PFASs) in Aqueous film-forming foam (AFFF) using ion-exchange and nonionic resins, Environ. Sci. Technol. 55 (2021) 5001–5011, https://doi.org/10.1021/acs.est.1c00769.

[20] R. Li, S. Alomari, T. Islamoglu, O.K. Farha, S. Fernando, S.M. Thagard, T.M. Holsen, M. Wriedt, Systematic study on the removal of per-and polyfluoroalkyl substances from contaminated groundwater using metal-organic frameworks, Environ. Sci. Technol. 55 (2021) 15162–15171, https://doi.org/10.1021/acs.est.1c03974.

[21] J. Huang, Y. Shi, J. Xu, J. Zheng, F. Zhu, X. Liu, G. Ouyang, Hollow covalent organic framework with "shell-confined" environment for the effective removal of anionic per- and polyfluoroalkyl substances, Adv. Funct. Mater. 32 (2022) 1–8, https://doi.org/10.1002/adfm.202203171.

[22] Q. Yu, R. Zhang, S. Deng, J. Huang, G. Yu, Sorption of perfluorooctane sulfonate and perfluorooctanoate on activated carbons and resin: Kinetic and isotherm study, Water Res. 43 (2009) 1150–1158, https://doi.org/10.1016/j.watres.2008.12.001.

[23] J. Yu, L. Lv, P. Lan, S. Zhang, B. Pan, W. Zhang, Effect of effluent organic matter on the adsorption of perfluorinated compounds onto activated carbon, J. Hazard. Mater. 225–226 (2012) 99–106, https://doi.org/10.1016/j.jhazmat.2012.04.073.

[24] N. Watanabe, M. Takata, S. Takemine, K. Yamamoto, Thermal mineralization behavior of PFOA, PFHxA, and PFOS during reactivation of granular activated carbon (GAC) in nitrogen atmosphere, Environ. Sci. Pollut. Res. 25 (2018) 7200–7205, https://doi.org/10.1007/s11356-015-5353-2.

[25] C. Ching, M.J. Klemes, B. Trang, W.R. Dichtel, D.E. Helbling, β-Cyclodextrin polymers with different cross-linkers and ion-exchange resins exhibit variable adsorption of anionic, zwitterionic, and nonionic PFASs, Environ. Sci. Technol. 54 (2020) 12693–12702, https://doi.org/10.1021/acs.est.0c04028.

[26] X. Qin, L. Bai, Y. Tan, L. Li, F. Song, Y. Wang, β-Cyclodextrin-crosslinked polymeric adsorbent for simultaneous removal and stepwise recovery of organic dyes and heavy metal ions: Fabrication, performance and mechanisms, Chem. Eng. J. 372 (2019) 1007–1018, https://doi.org/10.1016/j.cej.2019.05.006.

[27] W. Wang, H. Shao, S. Zhou, D. Zhu, X. Jiang, G. Yu, S. Deng, Rapid Removal of Perfluoroalkanesulfonates from Water by β-Cyclodextrin Covalent Organic Frameworks, ACS Appl. Mater. Interfaces 13 (2021) 48700–48708, https://doi.org/10.1021/acsami.1c14043.

[28] A. Yang, C. Ching, M. Easler, D.E. Helbling, W.R. Dichtel, Cyclodextrin polymers with nitrogen-containing tripodal crosslinkers for efficient PFAS adsorption, ACS Mater. Lett. 2 (2020) 1240–1245, https://doi.org/10.1021/acsmaterialslett.0c00240.

[29] R. Wang, Z.W. Lin, M.J. Klemes, M. Ateia, B. Trang, J. Wang, C. Ching, D. E. Helbling, W.R. Dichtel, A Tunable Porous β-Cyclodextrin Polymer Platform to Understand and Improve Anionic PFAS Removal, ACS Cent. Sci. 8 (2022) 663–669, https://doi.org/10.1021/acscentsci.2c00478.

[30] G. Crini, Review: a history of cyclodextrins, Chem. Rev. 114 (2014) 10940–10975, https://doi.org/10.1021/cr500081p.

[31] M. Verma, I. Lee, Y. Hong, V. Kumar, H. Kim, Multifunctional β-Cyclodextrin-EDTA-Chitosan polymer adsorbent synthesis for simultaneous removal of heavy metals and organic dyes from wastewater, Environ. Pollut. 292 (2022) 118447, https://doi.org/10.1016/j.envpol.2021.118447.

[32] M.V. Rekharsky, Y. Inoue, Complexation thermodynamics of cyclodextrins, Chem. Rev. 98 (1998) 1875–1917, https://doi.org/10.1021/cr970015o.

[33] M.J. Weiss-Errico, K.E. O'Shea, Detailed NMR investigation of cyclodextrin-perfluorinated surfactant interactions in aqueous media, J. Hazard. Mater. 329 (2017) 57–65, https://doi.org/10.1016/j.jhazmat.2017.01.017.

[34] Y. Ling, M.J. Klemes, L. Xiao, A. Alsbaiee, W.R. Dichtel, D.E. Helbling, Benchmarking Micropollutant Removal by Activated Carbon and Porous β-Cyclodextrin Polymers under Environmentally Relevant Scenarios, Environ. Sci. Technol. 51 (2017) 7590–7598, https://doi.org/10.1021/acs.est.7b00906.

[35] A. Alsbaiee, B.J. Smith, L. Xiao, Y. Ling, D.E. Helbling, W.R. Dichtel, Rapid removal of organic micropollutants from water by a porous β-cyclodextrin polymer, Nature 529 (2016) 190–194, https://doi.org/10.1038/nature16185.

[36] M.J. Klemes, Y. Ling, M. Chiapasco, A. Alsbaiee, D.E. Helbling, W.R. Dichtel, Phenolation of cyclodextrin polymers controls their lead and organic micropollutant adsorption, Chem. Sci. 9 (2018) 8883–8889, https://doi.org/10.1039/c8sc03267j.

[37] A. Choudhary, D. Dong, M. Tsianou, P. Alexandridis, D. Bedrov, Adsorption Mechanism of Perfluorooctanoate on Cyclodextrin-based Polymers: probing the Synergy of Electrostatic and Hydrophobic Interactions with Molecular Dynamics Simulations, ACS Mater. Lett. 4 (2022) 853–859, https://doi.org/10.1021/acsmaterialslett.2c00168.

[38] L. Chen, Y. Chen, H.G. Fu, Y. Liu, Reversible emitting anti-counterfeiting ink prepared by anthraquinone-modified β-cyclodextrin supramolecular polymer, Adv. Sci. 7 (2020), https://doi.org/10.1002/advs.202000803, 2000803 (1–8).

[39] J. Li, J. Wang, X. Yuan, Z. Wang, S. Sun, Q. Lyu, S. Hu, Efficient adsorption of BPA and Pb2+ by sulfhydryl-rich β-cyclodextrin polymers, Sep. Purif. Technol. 309 (2023) 122913, https://doi.org/10.1016/j.seppur.2022.122913.

[40] S. Murai, S. Imajo, Y. Takasu, K. Takahashi, K. Hattori, Removal of phthalic acid esters from aqueous solution by inclusion and adsorption on β-cyclodextrin, Environ. Sci. Technol. 32 (1998) 782–787, https://doi.org/10.1021/es970463d.

[41] J. Wang, Z.W. Lin, W.R. Dichtel, D.E. Helbling, Perfluoroalkyl acid adsorption by styrenic β-cyclodextrin polymers, anion-exchange resins, and activated carbon is inhibited by matrix constituents in different ways, Water Res. 260 (2024) 121897, https://doi.org/10.1016/j.watres.2024.121897.

[42] S. Lagergren, About the theory of so-called adsorption of soluble substances, Proc. r. Swedish Acad. Sci. 24 (1898) 1–39.

[43] Y.S. Ho, G. McKay, Pseudo-second order model for sorption processes, Process Biochem. 34 (1999) 451–465, https://doi.org/10.1016/S0032-9592(98)00112-5.

[44] J. Pala, T. Le, M. Kasula, M. Rabbani Esfahani, Systematic investigation of PFOS adsorption from water by Metal Organic Frameworks, Activated Carbon, Metal Organic Framework@Activated Carbon, and functionalized Metal Organic Frameworks, Sep. Purif. Technol. 309 (2023) 123025, https://doi.org/10.1016/j.seppur.2022.123025.

[45] R. Shahrokhi, A. Rahman, M.A. Hubbe, J. Park, Aminated clay-polymer composite as soil amendment for stabilizing the short- and long-chain per- and poly-fluoroalkyl substances in contaminated soil, J. Hazard. Mater. 472 (2024) 134470, https://doi.org/10.1016/j.jhazmat.2024.134470.

[46] M. Verma, I. Lee, S. Pandey, M. Nanda, V. Kumar, P.K. Chauhan, S. Kumar, M. S. Vlaskin, H. Kim, Bio-oil and biochar production from Ageratum conyzoides using triple-stage hydrothermal liquefaction and utilization of biochar in removal of multiple heavy metals from water, Chemosphere 340 (2023) 139858, https://doi.org/10.1016/J.CHEMOSPHERE.2023.139858.

[47] S. Deng, Y. Nie, Z. Du, Q. Huang, P. Meng, B. Wang, J. Huang, G. Yu, Enhanced adsorption of perfluorooctane sulfonate and perfluorooctanoate by bamboo-derived granular activated carbon, J. Hazard. Mater. 282 (2015) 150–157, https://doi.org/10.1016/j.jhazmat.2014.03.045.

[48] Drinking Water Quality Annual Report for Calendar Year 2022, Gwangju Air Base, 2023.

[49] W. Wang, X. Mi, H. Shi, X. Zhang, Z. Zhou, C. Li, D. Zhu, Adsorption behaviour and mechanism of the PFOS substitute OBS (sodium p-perfluorous nonenoxybenzene

sulfonate) on activated carbon, R. Soc. Open Sci. 6 (2019) 191069, https://doi.org/10.1098/rsos.191069.
[50] A.H. Karoyo, A.S. Borisov, L.D. Wilson, P. Hazendonk, Formation of host-guest complexes of β-cyclodextrin and perfluorooctanoic acid, J. Phys. Chem. B 115 (2011) 9511–9527, https://doi.org/10.1021/jp110806k.
[51] M.J. Weiss-Errico, I. Ghiviriga, K.E. O'Shea, 19F NMR characterization of the encapsulation of emerging perfluoroethercarboxylic acids by cyclodextrins, J. Phys. Chem. B 121 (2017) 8359–8366, https://doi.org/10.1021/acs.jpcb.7b05901.